Simultaneous measurement of two ultrashort laser pulses from a single spectrogram in a single shot

Daniel J. Kane

Southwest Sciences, Inc., 1570 Pacheco St., Suite E-11, Santa Fe, New Mexico 87505

G. Rodriguez and A. J. Taylor

Los Alamos National Laboratories, MS D429, Los Alamos, New Mexico 87545

Tracy Sharp Clement

JILA, University of Colorado, Boulder, Colorado 80309, National Institute of Standards and Technology, 325 Broadway, Boulder, Colorado 80303, and University of Colorado, Campus Box 440, Boulder, Colorado 80309

Received June 3, 1996; revised manuscript received September 3, 1996

Frequency-resolved optical gating (FROG) is a technique that produces a spectrogram of an ultrashort laser pulse. The intensity and phase of the ultrashort laser pulse can be determined through solving for the phase of the spectrogram with an iterative, phase-retrieval algorithm. This work presents a new phase-retrieval algorithm that retrieves both the probe and the gate pulses independently by converting the FROG phase-retrieval problem to an eigenvector problem. The new algorithm is robust and general. It is tested theoretically by use of synthetic data sets and experimentally by use of single-shot, polarization-gate FROG. We independently and simultaneously characterize the electric field amplitude and phase of a pulse (probe) that was passed though 200 mm of BK7 glass and the amplitude of an unchanged pulse (gate) from an amplified Ti:sapphire laser. When the effect of the 200 mm of BK7 glass was removed mathematically from the probe, there was good agreement between the measured gate and the calculated, prechirped probe. © 1997 Optical Society of America [S0740-3224(97)03204-9]

1. INTRODUCTION

Simple, reliable diagnostics have not been available to researchers who use and develop ultrafast laser systems. Some information about an ultrafast system being studied can be gleaned from optical methods such as simple autocorrelators, but questions arise: What is the intensity profile of the pulse? Should I add positive or negative group-velocity dispersion? Is the observed wing a satellite pulse or a wing? Interferometric autocorrelation[1] is an improvement to basic autocorrelation and provides more information about ultrafast pulse characteristics, but complete intensity and phase information about the pulse remain difficult to obtain. Indeed, simultaneous time and frequency information is required for retrieval of the full complex electric field.[2]

Time-frequency measurements of ultrashort pulses were first completed by Treacy in 1971.[3] His method disperses the input pulse in frequency, selects a portion of the frequency components to produce another pulse, then cross correlates the newly formed pulse with the original input pulse. Scanning the frequency filter over all the frequencies contained in the original pulse produces a three-dimensional plot of intensity versus frequency and time that is commonly referred to as a sonogram. This method was refined by Chilla and Martinez with the development of frequency-domain phase measurement, or FDPM.[4] Because the arrival time (i.e., the peak) of each frequency-filtered pulse is given by the derivative of the phase (in the frequency domain) with respect to frequency, they integrate to yield the phase of the pulse in the frequency domain. Coupling this result with the spectrum of the pulse gives the complex electric field in the frequency domain. The principal difficulty with this method is that if the peak of the arrival time of each frequency-selected pulse does not produce a function; as is the case with self-phase modulated pulses, the group delay is not well defined, and determination of the pulse is not possible.

Spectrograms are close relatives of sonograms. Rather than displaying the time arrival of frequency-filtered pulses, a spectrogram displays the frequency content of time slices of a pulse. Using optical methods to obtain a spectrogram of the pulse to be measured is the basis of a new technique for the complete characterization of ultrashort laser pulses called frequency-resolved optical gating[5–11] (FROG). FROG is a versatile technique that can be used in either multishot[5–7] or single-shot[8–11] geometries. A gate pulse, which can be virtually any duration, slices out portions of a probe pulse in the time domain using either an instantaneously responding, nonlinear ma-

0740-3224/97/040935-09$10.00

terial or a nearly instantaneously responding medium.[12] The sampled portion of the probe, or signal, is dispersed in a spectrometer. Like a sonogram, the resulting spectrogram contains all the intensity and phase information about the probe pulse.

Obtaining the spectrogram of a pulse is experimentally less complex than obtaining the sonogram; however, extracting the intensity and phase of a pulse from its spectrogram is mathematically more challenging. If an approach similar to that of Chilla and Martinez[4] is used to invert a spectrogram, the phase in the time domain is obtained, but the complete complex electric field is not. Because only the magnitude of the spectrogram can be measured, finding the full intensity and phase of the input pulse requires determining the spectrogram's phase, which places the FROG inversion problem into the category of two-dimensional, phase-retrieval problems.[8]

FROG assumes that the pulse gates itself; hence inversion of FROG traces is carried out assuming that the probe and the gate pulses are identical. Recent refinements using second-harmonic generation (SHG) FROG[13] extract the gate and the probe independently, without assuming identical probe and gate pulses, from a single spectrogram. This has the experimental advantage of allowing one to use an independent, unmeasured, and unrelated pulse of even a completely different frequency to measure another pulse. This technique, first demonstrated by DeLong *et al.*,[13] is analogous to a blind, two-dimensional deconvolution problem in which both the original function and the blurring function are unknown. Their technique, called twin retrieval of excitation electric fields FROG (TREEFROG), can be extended to all other experimental configurations, such as polarization gating. (FROG trace refers specifically to spectrograms produced when the probe pulse and the gate pulse are the same. TREEFROG trace refers to the general case of spectrograms produced when the probe pulse and the gate pulse are independent.)

In the present work the blind-FROG problem, or TREEFROG, is extended to the polarization-gate, single-shot geometry. Furthermore, a novel algorithm is introduced that uses an entirely new approach to obtain simultaneously both the probe and the gate from a single polarization-gate FROG spectrogram. The algorithm is robust and general. Two synthetic cases and an experimental case are presented as demonstrations. An error analysis of the experimental data shows the algorithm's ability to function in the presence of noise.

2. BACKGROUND

Polarization-gate FROG involves splitting a laser pulse and overlapping the two resulting pulses in an instantaneously responding $\chi^{(3)}$ medium. The probe pulse passes through the $\chi^{(3)}$ medium after it has first passed through a polarizer. When the gate and the probe interact in the nonlinear material, the gate pulse induces optical birefringence that rotates the polarization of the probe slightly, allowing a time slice of the probe to pass through a second, crossed polarizer. Any transmitted probe (signal) is spectrally resolved, and its intensity is measured as a function of wavelength and delay time, τ. For single-shot measurements, τ is mapped onto a spatial coordinate to yield FROG traces. Because of experimental simplicity, adaptability for single-shot use, and, most important, lack of ambiguity in time, one of the first FROG devices used the optical Kerr-effect in a polarization-gate arrangement.[9]

When optically induced birefringence is used as the nonlinear effect, the FROG spectrogram, $I_{\mathrm{FROG}}(\omega, \tau)$, is as follows:

$$I_{\mathrm{FROG}}(\omega, \tau) = \left| \int_{-\infty}^{\infty} E(t)|E(t-\tau)|^2 \exp(-i\omega t)\,\mathrm{d}t \right|^2, \tag{1}$$

where the gate and the probe pulses are identical. In the more general case of TREEFROG, the probe and the gate pulses are independent; $E(t)$ and $|E(t-\tau)|^2$ become $E_{\mathrm{Probe}}(t)$ and $E_{\mathrm{Gate}}(t-\tau)$. Unlike SHG TREEFROG, for which the intensity and phase of both the probe and the gate can be obtained, in the polarization-gate implementation of TREEFROG no phase information about the gate pulse can be obtained, because the gate is the *magnitude squared* of the gate pulse. However, polarization-gate TREEFROG has two advantages over SHG TREEFROG. There is no direction of time ambiguity, and spectral constraints are not needed to avoid other ambiguities.[13] The probe and the gate spectra do not need to be obtained simultaneously.

Since the FROG trace inversion problem is a two-dimensional phase-retrieval problem,[8] an iterative algorithm is required for finding the phase. Ideally each iteration of the algorithm results in a slightly better guess for the solution of the phase until convergence. How an algorithm determines each subsequent guess is paramount to its performance. The first FROG inversion algorithm used integration of $E(t)|E(t-\tau)|^2$ with respect to τ to obtain subsequent guesses for $E(t)$ (the so-called vanilla or basic algorithm).[8,14] While fast, this algorithm stagnates easily and fails to invert spectrograms of double pulses.[14,15] Much improvement in convergence properties was made when minimization of an error function[14] and the method of generalized projections[13,15,17] were employed to find each new guess for $E(t)$.

The algorithm used by DeLong *et al.* for TREEFROG to extract both the probe and the gate from a single FROG trace was based on the method of generalized projections.[13,15–17] Their algorithm uses initial guesses for $E_{\mathrm{Probe}}(t)$ and $E_{\mathrm{Gate}}(t)$ to generate a spectrogram, $E_{\mathrm{sig}}(\omega, \tau)$. During each iteration of the algorithm the magnitude of $E_{\mathrm{sig}}(\omega, \tau)$ is replaced by the square root of the experimentally measured TREEFROG trace. To generate the next guess for E_{Probe} and E_{Gate}, an inverse Fourier transform is performed to yield $E'_{\mathrm{sig}}(t, \tau)$. On even iterations the next guess for $E_{\mathrm{Probe}}(t)$ is determined by minimization of the error function:

$$Z = \sum_{t,\tau=1}^{N} |E'_{\mathrm{sig}}(t, \tau) - E_{\mathrm{Probe}}(t)E_{\mathrm{Gate}}(t-\tau)|^2 \tag{2}$$

with respect to $E_{\mathrm{Probe}}(t)$. On odd iterations a new guess for $E_{\mathrm{Gate}}(t)$ is found that minimizes the same error function but with respect to $E_{\mathrm{Gate}}(t)$. The algorithm is repeated until the error reaches an acceptable minimum.

For improved convergence of the algorithm for SHG TREEFROG, the spectra of both fields are used as an additional constraint.[13]

3. NEW ALGORITHM INTRODUCTION

Before the new inversion algorithm is discussed in detail, it is instructive to discuss the construction of TREEFROG (or FROG) traces by use of discrete vector pairs. This defines nomenclature that simplifies discussion of the algorithm. Two vectors of length N are used to represent the probe and the gate fields:

$$E_{\text{Probe}} = [E_1, E_2, E_3, E_4, \ldots, E_N],$$
$$E_{\text{Gate}} = [G_1, G_2, G_3, G_4, \ldots, G_N]. \tag{3}$$

The outer product of E_{Probe} and E_{Gate} is

$$\begin{bmatrix} E_1G_1 & E_1G_2 & E_1G_3 & E_1G_4 & \ldots & E_1G_N \\ E_2G_1 & E_2G_2 & E_2G_3 & E_2G_4 & \ldots & E_2G_N \\ E_3G_1 & E_3G_2 & E_3G_3 & E_3G_4 & \ldots & E_3G_N \\ E_4G_1 & E_4G_2 & E_4G_3 & E_4G_4 & \ldots & E_4G_N \\ \vdots & \vdots & \vdots & \vdots & \cdots & \vdots \\ \vdots & \vdots & \vdots & \vdots & \cdots & \vdots \\ \vdots & \vdots & \vdots & \vdots & \cdots & \vdots \\ E_NG_1 & E_NG_2 & E_NG_3 & E_NG_4 & \ldots & E_NG_N \end{bmatrix}. \tag{4}$$

This will be referred to as the *outer product form*.

The rows of the outer product form can be manipulated to generate an equivalent matrix that gives a time-domain representation of FROG trace. By leaving the first row unshifted and by shifting subsequent rows to the left, we obtain

$$\begin{bmatrix} E_1G_1 & E_1G_2 & E_1G_3 & \ldots & E_1G_{N-2} & E_1G_{N-1} & E_1G_N \\ E_2G_2 & E_2G_3 & E_2G_4 & \ldots & E_2G_{N-1} & E_2G_N & E_2G_1 \\ E_3G_3 & E_3G_4 & E_3G_5 & \ldots & E_3G_N & E_3G_1 & E_3G_2 \\ E_4G_4 & E_4G_5 & E_4G_6 & \ldots & E_4G_1 & E_4G_2 & E_4G_3 \\ \vdots & \vdots & \vdots & \vdots & \vdots & \vdots & \vdots \\ \vdots & \vdots & \vdots & \vdots & \vdots & \vdots & \vdots \\ \vdots & \vdots & \vdots & \vdots & \vdots & \vdots & \vdots \\ E_NG_N & E_NG_1 & E_NG_2 & \ldots & E_NG_{N-3} & E_NG_{N-2} & E_NG_{N-1} \\ \tau = 0 & \tau = -1 & \tau = -2 & \ldots & \tau = +3 & \tau = +2 & \tau = +1 \end{bmatrix}. \tag{5}$$

The $\tau = 0$ column is the first column, where τ is the time delay in resolution element number (column number). This is just the probe multiplied by the gate with no time shift between them. The next column is the $\tau = -1$ column, where the gate is delayed relative to the probe by one resolution element. After some column manipulation, the most negative τ is on the left and the most positive on the right; this *time-domain TREEFROG trace*, Eq. (5), is the discrete version of the product $E_{\text{Probe}}(t)E_{\text{Gate}}(t - \tau)$. The columns are constant in τ (delay) while the rows are constant in t (time). To obtain the TREEFROG trace, the Fourier transform of the product $E_{\text{Probe}}(t)E_{\text{Gate}}(t - \tau)$ with respect to t must be obtained. Each column of the matrix shown in Eq. (5) is Fourier transformed using a fast Fourier transform algorithm. The final step of taking the magnitude of the complex result produces the TREEFROG trace.

4. NEW ALGORITHM INVERSION

While there are an infinite number of complex *images* that have the same magnitude as the TREEFROG trace we wish to invert, there is only one image that can be formed by the outer product of a *single pair of vectors* that has the same magnitude as the TREEFROG trace to be inverted. As in other two-dimensional phase-retrieval algorithms, to find the proper vector pair we use an iterative algorithm (Fig. 1). An initial guess for the phase of the TREEFROG trace is made, and the result is decomposed into outer products. The principal pair of vectors is kept and used to determine the next guess of the TREEFROG trace phase.

To construct the initial guess for the phase, a TREEFROG trace is constructed by vector pairs, one complex (probe) and, in the case of polarization-gate TREEFROG, one real (gate) that are both random-noise modulated by a broad Gaussian. The iterative algorithm starts with replacing the magnitude of the newly constructed TREEFROG trace by the square root of the magnitude of the experimental TREEFROG trace.

The TREEFROG trace with the correct magnitude is converted to the time-domain TREEFROG trace [Eq. (5)] by use of an inverse Fourier transform by column (see Fig. 1). Next the time-domain TREEFROG trace is converted to the outer product form [Eq. (4)]. If the intensity and phase of the TREEFROG trace are correct, this matrix is a matrix of rank 1. That is, it would have one and *only one* nonzero eigenvalue. The eigenvector corresponding to this eigenvalue spans the range of the outer product matrix and is called the right eigenvector; this vector is the probe. The complex conjugate of the eigenvector of the transpose of the outer product matrix (left eigenvector) is the gate.

Unfortunately, the outer product form matrix produced by the initial guess has several eigenvectors. In fact, although it may be an ill-conditioned matrix, it will probably not be singular. The range of this new matrix is no longer a single line in N space, but rather an ellipsoid in N space. The question arises, Which eigenvector pair (right and left) represents the best next guess for the

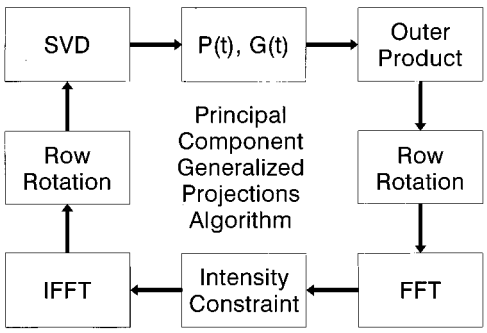

Fig. 1. Schematic of the FROG PCGPA presented in this paper. $P(t)$ and $G(t)$ refer to E_{Probe} and E_{Gate}, respectively.

probe and the gate? We know from linear algebra that the eigenvectors span the range of the outer product form matrix, and they are linearly independent although not necessarily orthogonal. This means that the best next guess may actually be a superposition of two or more different, but linearly independent, eigenvectors.

The problem of producing the next best guess is solved by an elegant numerical method in linear algebra called a singular value decomposition (SVD).[18,19] SVD decomposes a matrix into a superposition of outer products of vectors. This can be written as

$$\mathbf{A} = \mathbf{U} \times \mathbf{W} \times \mathbf{V}^T, \tag{6}$$

where $\mathbf{U}$ and $\mathbf{V}^T$ are orthogonal square matrices and $\mathbf{W}$ is a square diagonal matrix. Because both $\mathbf{U}$ and $\mathbf{V}$ are orthogonal, the column vectors of these matrices are all orthogonal and form an orthonormal basis set that describes the range of matrix $\mathbf{A}$. Thus the matrix $\mathbf{A}$, the outer product form, is decomposed into a superposition of outer products between probe vectors (columns of $\mathbf{U}$) and gate vectors (rows of $\mathbf{V}^T$). The diagonal values in $\mathbf{W}$ (the only nonzero elements of $\mathbf{W}$) determine the relative weights of each outer product and therefore how much each outer product contributes to matrix $\mathbf{A}$. In the blind-FROG retrieval algorithm presented here, only the outer product pair with the largest weighting factor, or the *principal component*, is kept for the next iteration of the algorithm. The remaining columns of $\mathbf{U}$ and $\mathbf{V}$ contain little information.

A new TREEFROG trace is constructed from the probe vector and the magnitude of the gate vector obtained from the SVD of the outer product form matrix. The process is repeated (see Fig. 1) until the TREEFROG trace error, ϵ_{TF} (analogous to the FROG trace error[8]), reaches an acceptable minimum:

$$\epsilon_{\mathrm{TF}} \equiv \left[\frac{1}{N^2} \sum_{i=1}^{N} \sum_{j=1}^{N} [I_{\mathrm{TF}}(\omega_i, \tau_j) - I_{\mathrm{MEASURED}}(\omega_i, \tau_j)]^2 \right]^{1/2}, \tag{7}$$

where ϵ_{TF} represents the per-element rms error of the TREEFROG trace, $I_{\mathrm{TF}}(\omega_i, \tau_j)$ is the current iteration of the TREEFROG trace, $I_{\mathrm{MEASURED}}(\omega_i, \tau_j)$ is the measured TREEFROG trace, and ω_i and τ_j are the ith frequency and the jth delay in the frequency and the delay vectors, respectively.[13]

Using SVD has an additional advantage as well. SVD provides the best packing efficiency for a given image.[18] In other words, the image produced from the product of the outer product of the vector pair with the largest weighting factor is the best rank 1 approximation of that image in the least-squares sense. That is, it minimizes the error function[18]

$$\epsilon^2 = \sum_{i,j=1}^{N} |E^{i,j}_{\mathrm{Outer}} - E^{i}_{\mathrm{Probe}} E^{j}_{\mathrm{Gate}}|^2 \tag{8}$$

where E_{Outer} is the outer product form of the TREEFROG trace shown in Eq. (4), E_{Probe} is the probe vector, E_{Gate} is the gate vector, and ϵ is the error. This shows that the probe and gate found by SVD in the algorithm described above represent a projection[13,15–17] found directly without minimization. Neither the set of functions with a given Fourier transform magnitude nor the set of all outer products is a convex set, however. Because one or more of the constraints applied is not a projection onto a convex set, this algorithm is related to the technique known as generalized projections; hence we call this algorithm a principal component generalized projections algorithm, or PCGPA. Like the generalized projections algorithm used by DeLong *et al.*, convergence is not assured.[15,16] In practice, however, the algorithm performs well and is very robust.

Faster convergence can sometimes be achieved by rotation of the principal vector pair slightly by addition of a superposition of some of the minor vectors. This is accomplished by use of a multivariate minimization in which one minimizes ϵ_{TF} by changing the weighting factors in the superposition. Currently only a single variable minimization has been implemented, in which the next guess for the probe and gate is computed from a linear superposition of the principal vector pair and the first minor right and left eigenvector pair. The high-level math package (MATLAB) used to implement PCGPA with a single variable minimization ran too slowly (several minutes per iteration) when attempting a multivariate minimization and provided no improvement in convergence.

5. SYNTHETIC DATA TESTS

While a variety of algorithms can be used to extract the original pulses from FROG and TREEFROG traces, they must converge to be useful. This section describes two tests of the new algorithm in which theoretical spectrograms are used. The first test uses a double pulse, which is a standard test for FROG phase-retrieval algorithms.[14,15] It consists of a coherent sum of two Gaussian pulses separated by twice their intensity full width at half-maximum with no phase distortion. A FROG trace of this double pulse is shown in Fig. 2(a). The curve in Fig. 2(b) shows the intensity of the original pulse, and the ×'s show the intensity of the retrieved probe with an $\epsilon_{\mathrm{TF}} < 10^{-4}$. The gate pulse used was identical to the probe pulse. Figure 2(c) shows that the retrieved gate pulse intensity (×'s) is identical to the original gate pulse intensity (curve). The ×'s in Fig. 2(d) show that the frequency deviation of the retrieved probe closely matches the curve showing the frequency devia-

tion of the original probe, except near the edges, where the intensity is nearly zero and the phase is not well defined. Figure 3 shows the convergence history for the double pulse test. The TREEFROG algorithm converges to an $\epsilon_{TF} < 10^{-4}$ in 55 iterations.

Figure 4 shows the results of a more pathological test case. The test pulses for the probe and the gate are different and are shown as curves in Figs. 4(b) and 4(c), respectively. These pulses are random-noise modulated by a Gaussian and filtered to remove all frequencies greater

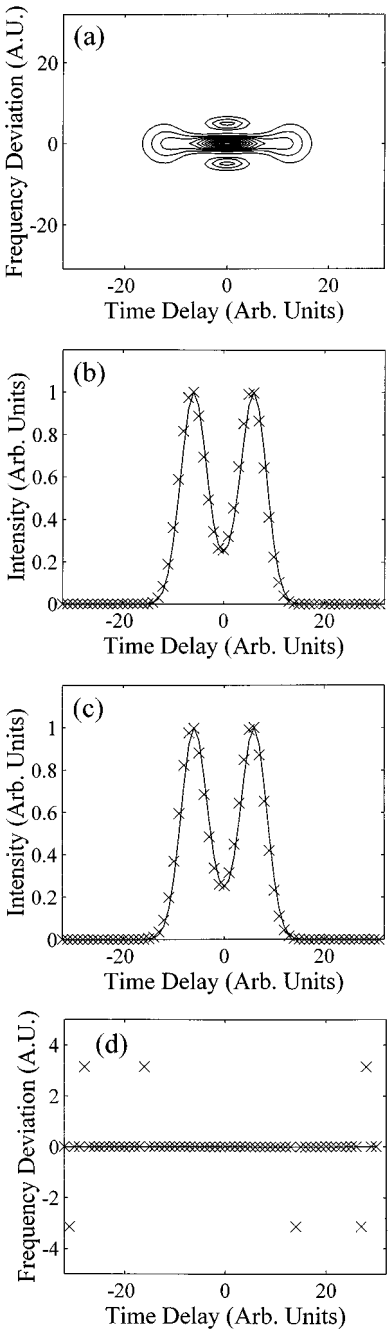

Fig. 2. (a) FROG trace of the double pulse used for the algorithm test. (b) Solid curve, the original probe intensity; ×'s, retrieved probe intensity. (c) Solid curve, gate intensity; ×'s, retrieved gate intensity. (d) Solid curve, frequency deviation of the original probe pulse; ×'s, frequency deviation of the retrieved probe pulse.

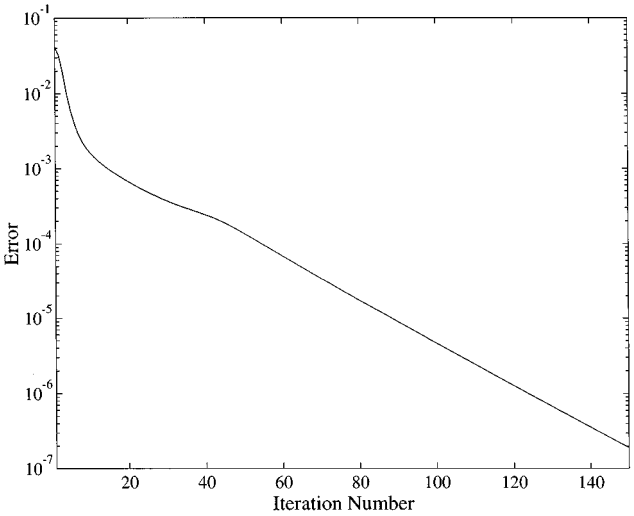

Fig. 3. Semi-log plot showing the error history of the PCGPA when retrieving the probe and gate from the spectrogram shown in Fig. 2(a).

than 0.8 of the Nyquist limit. A TREEFROG trace of the pulses is shown in Fig. 4(a). It is highly distorted and contains frequencies up to the Nyquist limit. In spite of this, the algorithm faithfully reproduced both the probe [Fig. 4(b), ×'s] and the gate [Fig. 4(c), ×'s]. Even the frequency deviation of the probe pulse [Fig. 4(d)] is shown to be accurately reproduced.

6. EXPERIMENTAL TEST

Experiments were conducted as a further test of both the algorithm presented in this work and of polarization-gated TREEFROG. To produce two different pulses that could still be compared directly, the probe pulse was lengthened by being dispersed in 200 mm of BK7 glass while the gate pulse was not dispersed. The phase distortion resulting from the BK7 glass was mathematically removed from the measured probe pulse. The intensity profile of the result closely matched the measured gate pulse.

The experiments were performed at the Los Alamos National Laboratories with an ultrashort pulse Ti:sapphire laser at the Bright Source.[20] This laser is a 5-Hz system that can amplify pulses to >50 mJ at 810 nm. The output of the oscillator is stretched by a two-grating stretcher and amplified by a Ti:sapphire regenerative amplifier. The pulses are further amplified in Ti:sapphire rods pumped by a frequency-doubled Nd glass laser. The final output is recompressed in a two-grating compressor to provide ~50 mJ pulses with durations of 160–200 fs. For the experiments presented in this paper, the last amplifier stage was not used, reducing the final output to ~10 mJ. A beam splitter sent approximately 1 mJ to an attenuator just before the FROG unit. The final input energy to the FROG device was approximately 200 μJ. A single-shot autocorrelator was used to monitor the output and showed wings on the output pulses.

A schematic diagram of the modified, single-shot, polarization-gate FROG device is shown in Fig. 5. A beam splitter divides the input beam into two replicas.

The probe beam passes through two large BK7 right-angle prisms (total path of 200 mm) to disperse and lengthen the probe pulse by 200%–300%. It is then polarized at 45° relative to the gate beam by a calcite polarizer with an attenuation of >58 dB. The beams are focused with a 10-cm focal-length cylindrical lens and cross at an angle of 7° within a quartz window that acts as the instantaneous, nonlinear medium. The probe beam is sent into a crossed calcite polarizer (attenuation >58 dB), and the transmitted signal is imaged onto the slits of a SPEX imaging spectrometer. At the focal plane of the spectrometer is an uncooled Electrim EDC 1000HR CCD camera (included with the camera is an 8-bit digitizer and computer interface). Since the quantum efficiency of silicon CCD arrays is high at 810 nm, this camera was adequate.

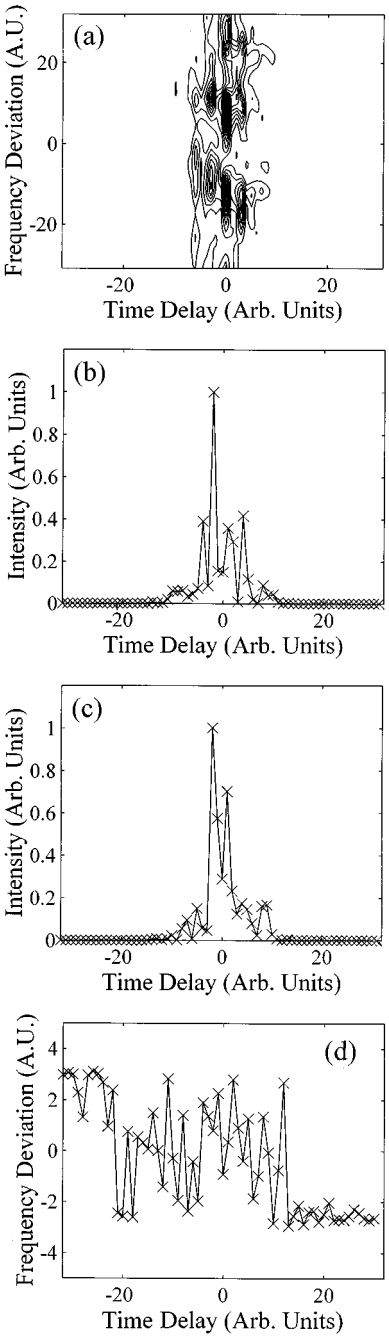

Fig. 4. (a) TREEFROG trace formed from the probe, depicted in parts (b) and (d), and the gate, depicted in part (c). (b) Solid curve, original probe intensity; ×'s, retrieved probe intensity. (c) Solid curve, gate intensity; ×'s, retrieved gate intensity. (d) Solid curve, frequency deviation of the original probe pulse; ×'s, frequency deviation of the retrieved probe pulse.

The blind-FROG trace for this experiment is shown in Fig. 6(a). The trace is tilted to the right, indicating that the probe pulse has positive linear chirp. (Only the probe affects the tilt of the trace because the gate is the magnitude squared of the gate pulse.) The correlation between the intensity of the probe and the squared intensity of the gate, which can be determined by integration along the frequency axis of the FROG trace, has a FWHM of ~525 fs.

The raw FROG trace directly from the camera was a 753×244 array. Every 3 pixels across the camera were binned, resulting in a 251×244 array. The rows and columns were filtered to remove all frequencies greater than 50% of the Nyquist limit (to prevent aliasing when resampling the array), the constant background was removed, and the array was resampled down to a 64×64 array.[8] This array was input into the algorithm that converged to $\epsilon_{\mathrm{TF}} < 1\%$ in fewer than 20 iterations (~2 min in the MATLAB environment with a 486 DX/2 66 MHz personal computer). Figure 7 shows the measured probe pulse, the measured gate pulse, and the results of a calculation to determine how the probe would have appeared before the 200 mm of glass (called "Calculated Gate" in the figure). There is excellent agreement between the gate pulse and the probe pulse with the effects of the BK7 computationally removed, providing another successful test of polarization-gate TREEFROG and the algorithm presented in this paper.

7. ERROR ANALYSIS

Effects of noise on the inversion of FROG traces have been investigated previously with a different algorithm.[21] That discussion concentrated on the global effects of noise on a few specific FROG traces, and generalizations to all FROG traces were made concerning the final error of the retrieved pulse and the convergence criteria for the algorithm. The error analysis presented in this work is intended to determine how accurately a specific pulse is obtained from an experimental TREEFROG trace and how well, in general, the new algorithm functions in the presence of noise. The confidence limits on the extracted probe and gate pulses were obtained with a Monte Carlo simulation of synthetic data sets.[19]

The probe and gate extracted from the experimental TREEFROG trace will be called p_0 and g_0, respectively; they may differ slightly from the actual probe and gate, p_{true} and g_{true}. Hence confidence limits for p_0 and g_0 must be determined. To accomplish this, 100 new TREEFROG traces were constructed from p_0 and g_0 that were corrupted by both additive and multiplicative noise representative of the noise levels on the original, experimental, TREEFROG trace. Each noisy TREEFROG trace, I_{NOISY}, is given by:

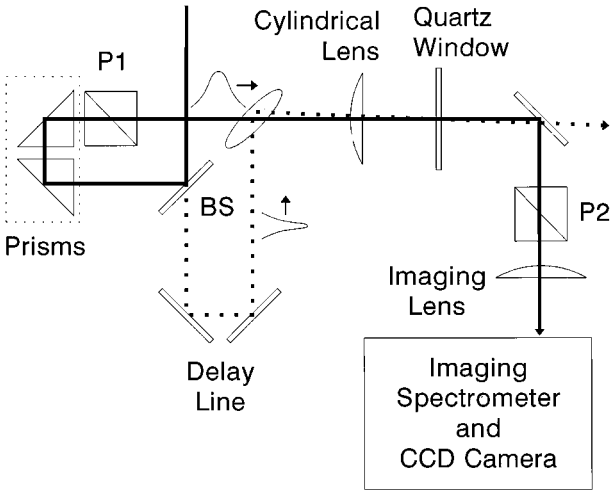

Fig. 5. Schematic of the modified FROG device used in this work. Prisms were used instead of turning mirrors to add dispersion to the probe. The pump (dotted line) is sent to a delay line and is sent below the probe. Both beams are focused with a cylindrical lens and are combined in a quartz window acting as the nonlinear medium. The interaction region is imaged onto the slits of an imaging spectrometer.

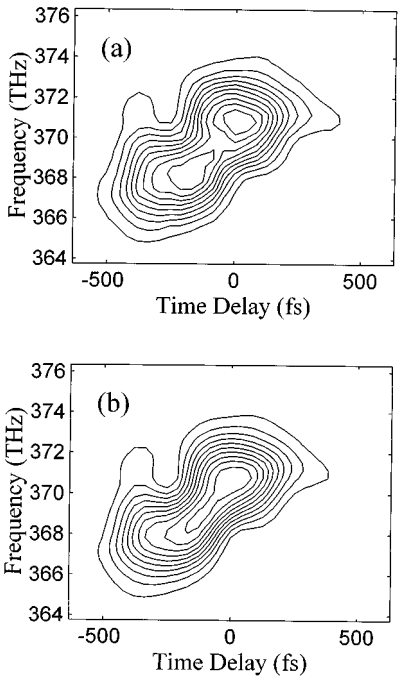

Fig. 6. (a) TREEFROG trace obtained in this experiment. (b) TREEFROG trace reconstructed from the probe and gate extracted from the experimental TREEFROG trace shown in (a).

$$I^{ij}_{\mathrm{NOISY}} = I^{ij}_{\mathrm{TF}}(1 + m^{ij}) + \max(I^{ij}_{\mathrm{TF}})a^{ij}, \qquad (9)$$

where I_{NOISY} is the noisy TREEFROG trace, I_{TF} is the original, uncorrupted TREEFROG trace, m is the multiplicative noise constant, and a is the additive noise constant. $\mathrm{Max}(I^{ij}_{\mathrm{TF}})$ is the maximum value of the TREEFROG trace I_{TF}. The constants m^{ij} and a^{ij} were varied randomly about zero with a normalized width of 0.04 and 0.015, respectively. The algorithm was applied to each of the 100 noise-corrupted TREEFROG traces for 100 iterations. The probe and gate giving the minimum ϵ_{TF} were kept; these minima ranged between 0.014 and 0.023, yielding 100 slightly different probe and gate pairs.

The results are summarized in Figure 8. The solid curves in Figs. 8(a) and 8(c) depict the intensity of the probe (p_0) and the gate (g_0) pulses, respectively. The error bars are the standard deviation of the intensity found in the set of 100 probe and gate pulses obtained from the noise-corrupted TREEFROG traces. The phase of each of the 100 probe pulses contained a random offset. Consequently, the calculated phases were differentiated with respect to time so that they could be compared directly from pulse to pulse. Figure 8(b) shows a plot of the frequency deviation of p_0 with error bars that given by the standard deviation of the frequency deviation. In an interesting aside, the error shown for the peak of the probe intensity is due largely to the uncertainty of time zero for the pulse. The frequency deviation showed no such error. Even though the entire intensity profile shifts slightly about zero (about one pixel) from pulse to pulse, the instantaneous frequency does not. Therefore there is an uncertainty of the phase relative to the intensity when noise is present.

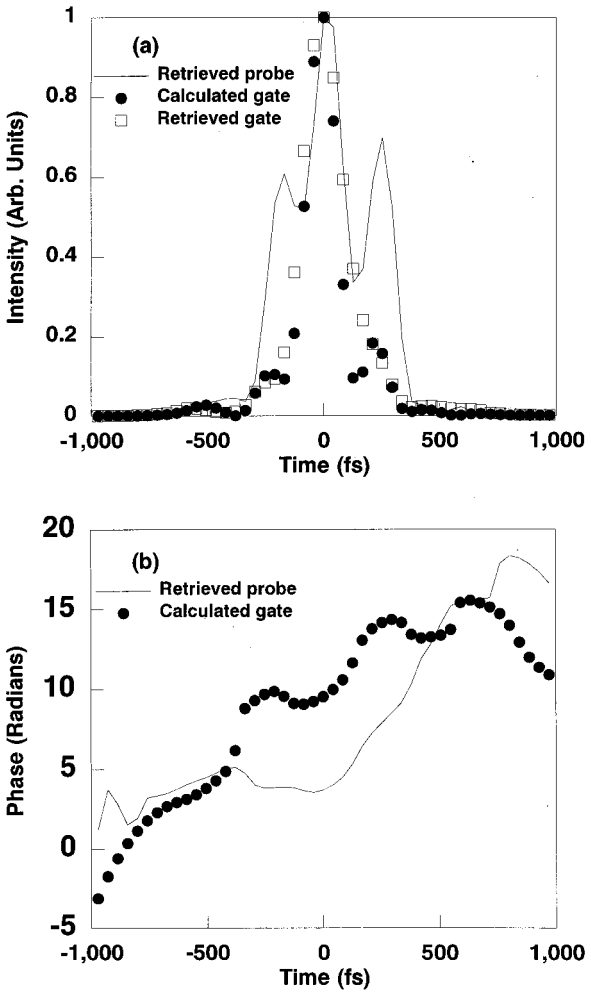

Fig. 7. (a) Intensity profiles of the pulses. The calculated gate is how the probe pulse would appear before the added BK7 glass with the dispersion removed mathematically. (b) Phases of the retrieved probe pulse and the calculated gate pulse.

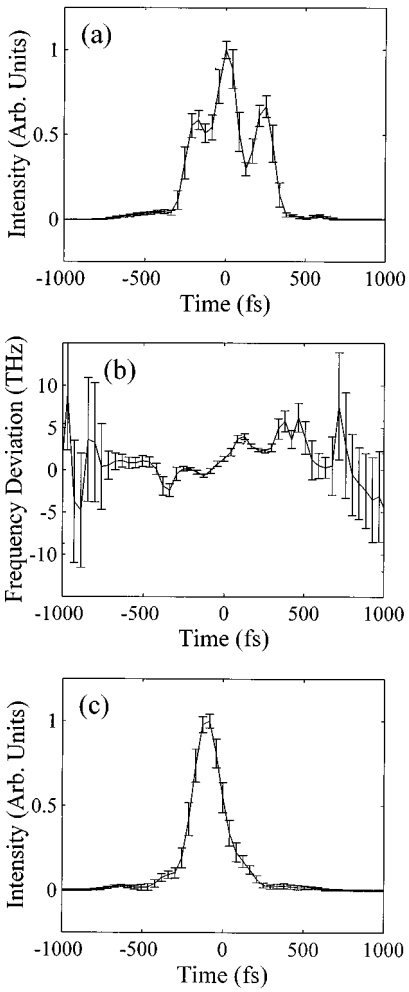

Fig. 8. Results of the error analysis for the probe and gate shown in Fig. 4.

8. POLARIZATION-GATE TREEFROG PITFALLS

One pitfall of using polarization-gate blind FROG is that when there are no phase distortions present in the probe the TREEFROG trace does not change when the probe and gate are interchanged. As a result any TREEFROG algorithm may converge with the probe and gate reversed. Even minor phase distortions in the probe can prevent this from occurring. However, this seems to be a minor problem.

Of more concern is that polarization-gate TREEFROG has an algorithm-independent effective ambiguity when the pulse shapes and durations of the probe and gate are similar. It occurs because ϵ_{TF} changes very little as the pulse widths of the probe and gate change in opposite directions. For example, a TREEFROG trace produced by a Gaussian probe pulse with a FWHM of 100 fs and a Gaussian gate (the actual gate, not the gate pulse) with the same FWHM will differ from the TREEFROG trace produced by a Gaussian probe pulse with a FWHM of 105 fs and a Gaussian gate with a FWHM of 95 fs by an ϵ_{TF} of only 0.00038. Subtle differences that are present can be obscured by noise. On the other hand, if the probe and gate have different shapes and very different widths, as they do in the experiments described here, effective ambiguities do not appear to be a problem.

9. CONCLUSIONS

A new phase-retrieval algorithm to invert TREEFROG and FROG traces, has been developed that obtains the probe and gate pulses independently. This new algorithm, principal component generalized projections (PCGPA), is robust and converges quickly. It useful in a variety of experimental configurations.

The PCGPA has been demonstrated for both theoretical and experimental data. The theoretical data include a double pulse—a very difficult test case for FROG inversion algorithms.[14,15] The experimental data measured the intensity and phase of a pulse that has been chirped by passing though a known quantity of dispersant and the intensity of a pulse that was unchanged. When the added glass was removed mathematically from the dispersed probe pulse, its intensity profile agreed well with the intensity profile of the measured gate pulse.

Because of the additional constraint of a real gate, polarization-gate TREEFROG does not require spectral constraints for proper operation of the PCGPA, provided the aforementioned precautions concerning effective ambiguities are observed. By removing the real constraint on the gate, that is, by removing the step of taking the absolute value of the gate after the SVD step, PCGPA can be used in other FROG geometries such as SHG TREEFROG and self-diffraction TREEFROG. The algorithm would converge properly, although more slowly (more iterations required); however, severe ambiguities might occur in any spectrogram inversion that produces unrelated, complex-valued probe and gate pulses, such as SHG and self-diffraction TREEFROG. (Interestingly, by constraining the gate to be a function of the probe, as in FROG inversions, all ambiguities appear to be removed.) It is not difficult to obtain several similar, yet distinct, complex-valued probe–gate combinations from a single TREEFROG trace. Initial tests indicate that in some cases this may be remedied by the addition of a spectral constraint step to the PCGPA: After the SVD step (see Fig. 1), the magnitude of the Fourier transform of either the probe or the gate fields is replaced by the square root of its respective spectra. However, applying it in this manner has not been comprehensively tested and represents work in progress.

Sonograms can also be inverted with the PCGPA as long as it is known whether the full complex gate or only the magnitude of the gate is required for the construction of the sonogram. Input and output are in the frequency domain, whereas the magnitude-replacement constraint is applied in the time domain. Indeed, any sonogram or spectrogram, regardless of whether it was formed optically or otherwise, can be inverted with this algorithm.

ACKNOWLEDGMENTS

Daniel J. Kane would like to acknowledge the support of National Science Foundation grant III-9361715. The au-

thors would also like to thank Rick Trebino and Ken DeLong for their helpful discussions and David Bomse for his editorial suggestions.

REFERENCES

1. J.-C. Diels, J. J. Fontaine, and W. Rudolph, "Ultrafast diagnostics," Revue Phys. Appl. **22** 1605–1611 (1987).
2. V. Wong and I. A. Walmsley, "Linear filter analysis of methods for ultrashort-pulse-shape measurements," J. Opt. Soc. Am. B **12**, 1491–1499 (1995).
3. E. B. Treacy, "Measurement and interpretation of dynamic spectrograms of picosecond light pulses," J. Appl. Phys. **42**, 3848–3858 (1971).
4. J. L. A. Chilla and O. E. Martinez, "Analysis of a method of phase measurement of ultrashort pulses in the frequency domain," IEEE J. Quantum Electron. **27**, 1228–1235 (1991).
5. D. J. Kane and R. Trebino, "Characterization of arbitrary femtosecond pulses using frequency-resolved optical gating," IEEE J. Quantum Electron. **29**, 571 (1993).
6. K. W. DeLong, R. Trebino, J. Hunter, and W. E. White, "Frequency-resolved optical gating with the use of second-harmonic generation," J. Opt. Soc. Am. B **11**, 2206–2215 (1994).
7. J. Paye, M. Ramaswamy, J. G. Fujimoto, and E. Ippen, "Measurement of the amplitude and phase of ultrashort light pulses from spectrally resolved autocorrelation," Opt. Lett. **18**, 1946–1948 (1993).
8. R. Trebino and D. J. Kane, "Using phase retrieval to measure the intensity and phase of ultrashort pulses: frequency-resolved optical gating," J. Opt. Soc. Am. A **10**, 1101–1111 (1993).
9. D. J. Kane, and R. Trebino, "Single-shot measurement of the intensity and phase of an arbitrary ultrashort pulse by using frequency-resolved optical gating," Opt. Lett. **18**, 823–825 (1993).
10. D. J. Kane, A. J. Taylor, R. Trebino, and K. W. DeLong, "Single-shot measurement of the intensity and phase of a femtosecond UV laser pulse with frequency-resolved optical gating," Opt. Lett. **19**, 1061–1063 (1994).
11. T. S. Clement, A. J. Taylor, and D. J. Kane, "Single-shot measurement of the amplitude and phase of ultrashort laser pulses in the violet," Opt. Lett. **20**, 70–72 (1995).
12. K. W. DeLong, C. L. Ladera, R. Trebino, B. Kohler, and K. R. Wilson, "Ultrafast-pulse measurement using noninstantaneous nonlinearities: Raman effects in frequency-resolved optical gating," Opt. Lett. **20**, 486–488 (1995).
13. K. W. DeLong, R. Trebino, and W. E. White, "Simultaneous recovery of two ultrashort laser pulses from a single spectrogram," J. Opt. Soc. Am. B **12**, 2463–2466 (1995).
14. K. W. DeLong and R. Trebino, "Improved ultrashort pulse-retrieval algorithm for frequency-resolved optical gating," J. Opt. Soc. Am. A **11**, 2429–2437 (1994).
15. K. W. DeLong, D. N. Fittinghoff, R. Trebino, B. Kohler, and K. Wilson, "Pulse retrieval in frequency-resolved optical gating based on the method of generalize projections," Opt. Lett. **19**, 2152–2154 (1994).
16. E. Yudilevich, A. Levi, G. J. Habetler, and H. Stark, "Restoration of signals from their signed Fourier transform magnitude by the method of generalized projections," J. Opt. Soc. Am. A **4**, 236–246 (1987).
17. Y. Yang, N. P. Galatsanos, and H. Stark, "Projection-based blind deconvolution," J. Opt. Soc. Am. A **11**, 2401–2409 (1994).
18. A. Jain, *Fundamentals of Digital Image Processing* (Prentice-Hall, Englewood Cliffs, N.J., 1992).
19. W. H. Press, W. T. Vetterling, S. A. Teukolsky, and B. R. Flannery, *Numerical Recipes in FORTRAN: the Art of Scientific Computing*, 2nd ed. (Cambridge U. Press, Cambridge, 1992).
20. G. Rodriguez, J. P. Roberts, and A. J. Taylor, "Ultraviolet ultrafast pump-probe laser based on a Ti:sapphire laser system," Opt. Lett. **19**, 1146 (1994).
21. D. N. Fittinghoff, K. W. DeLong, R. Trebino, and C. L. Ladera, "Noise sensitivity in frequency-resolved optical-gating measurements of ultrashort laser pulses," J. Opt. Soc. Am. B **12**, 1955–1967 (1995).